

# MECHANISMS OF ACOUSTIC SURFACE WAVE GENERATION BY RIGID CYLINDER ARRAYS

DL Berry,  
Escola de Ciência e Tecnologia, Universidade de Évora, 7002-554 Évora, Portugal

S Taherzadeh and K Attenborough  
School of Engineering and Innovation, The Open University, Milton Keynes, UK

## 1 INTRODUCTION

Classical theories for a point source in air above a surface with an impedance having an imaginary part much larger than the real part (such as that of a thin porous layer over a hard boundary) predict the occurrence of an airborne surface wave near grazing incidence [1]. Raspert and Baird [2] demonstrated that the surface wave arising from a point source above an impedance plane is an independently propagating wave.

The propagation of audio-frequency sound waves over hard surfaces is affected significantly if they are rough. Tolstoy [3,4] and Twersky [5] have derived theories for surface wave generation above randomly and periodically rough boundaries. Consistent with the expected behaviour, surface waves due to a point source in air over a rough surface are characterised by cylindrical spreading with increasing range in the horizontal plane, exponential decay with increasing height above the plane, and a reduced phase velocity  $v < c$ , where  $c$  is the speed of sound in air.

Airborne surface waves have been measured over arrays of thin aluminium strips mounted on a rigid sheet of plywood [6], lattices of square cavities constructed from overhead lighting panels mounted on a wooden board [7], rectangular strips on a hard surface [8] and a comb-like structure [9,10]. Allard, Lauriks, and Kelders [11-13] investigated ultrasonic surface wave generation over triangular-grooves, rectangular grooves, a doubly periodic grating, and honeycomb surfaces. Tolstoy [3] and Twersky [5] produced models for effective impedance of semi-cylindrical elements placed on a rigid flat surface. Boulanger et al [14] extended these models to roughness shapes other than semi-cylindrical cross section by including a hydraulic shape factor and compared resulting predictions with measurements. While there was agreement between the model predictions and measurements for semi-cylindrical elements, comparisons of predictions with data for other shapes (triangular and rectangular elements) were less satisfactory. Also, the influence of roughness in the form of low walls and lattice arrangements on outdoor propagation has been investigated in the context of using deliberately introduced roughness for surface transport noise control [15]. So far, neither propagation over arrays of cylinders on a hard plane nor the way in which surface waves are generated over periodically rough surfaces have been investigated to any extent.

In this study we simulate the propagation of short acoustic pulses above evenly spaced cylinders on a rigid plane and study the nature of the predicted waveform following the main pulse arrival to investigate the possible generation of surface waves. Here we use the formulation of Boulanger et al [14] to determine the spatial dependence of the acoustic pressure waveforms produced by cylinder arrays on a rigid plane, and present results for the influence of source-array-receiver geometries and of configurations and sizes of cylinders both in the time and frequency domain.

We show that in the time domain, this field comprises a direct contribution and a separate delayed "tail" as a result of scattering from the cylinders and reflection from the plane boundary, its persistence depending upon the arrangement (spacing and size) of the cylinders. Fourier analysis of this tail shows that, for loosely distributed cylinders, it is composed of a series of spectral peaks resulting from constructive interference consistent with Bragg diffraction theory and amplitudes depending on the number density and size of the cylinders. For compactly distributed cylinders, the lowest frequency peak is consistent with a quarter wavelength "organ pipe" resonance between the

cylinders. We also show that at the resonance frequencies the total field is confined to a region just above the cylinder array. It also demonstrates the characteristics of a surface wave.

In Section 2 we present a brief description of the multiple scattering theory used in this study for the spatial dependence of the acoustic pressure waveforms produced for different source-receiver geometries and different configurations and sizes of cylinders on a rigid plane. Using this theory, we explore, in Section 3, how such irregular surfaces affect the propagation of acoustic pulses - and in this case, the propagation of delta pulses of infinitely short length corresponding to a flat, infinitely-wide, frequency spectrum. Specifically, we analyse the pulse tails i.e., the parts of the waveform after the main arrival at the receiver resulting from the interaction of the pulse with the cylinders and rigid surface. Finally, Section 4 discusses this study in the light of previous work on acoustic propagation over periodically-rough surfaces.

## 2 THEORY

The characteristics of sound propagating over cylinders on a rigid plane has been explored here using a treatment similar to that of Boulanger et al [14] who considered the propagation of cylindrical waves over finite impedance *semi*-cylinders on a smooth acoustically hard surface. This treatment, using a semi-analytical Multiple Scattering Theory (MST) and based on the work of Linton et al [16], demonstrated success in modelling such systems proving good agreement with experimental measurements.

Consider a cylindrical wave incident on an array of rigid cylinders placed on a flat hard plane and arranged perpendicularly to the direction of propagation - see Figure (1). The polar coordinates of the field point in the Cartesian reference frame  $(Ox, Oy)$  are represented by  $(r, \theta)$ , and the polar coordinates of the field point in the reference frame  $(O_jx, O_jy)$  centred at the  $j$ th cylinder centre,  $O_j(x_j, y_j)$ , are represented by  $(r_j, \theta_j)$ .

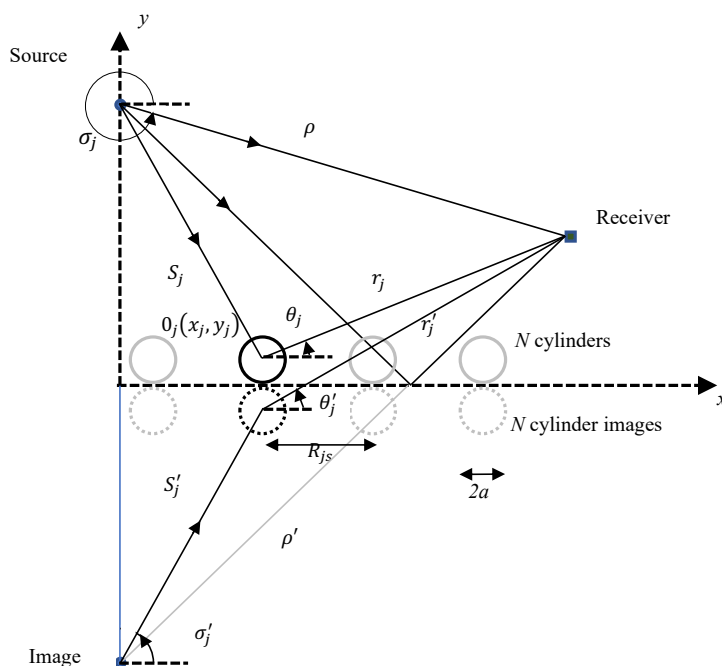


Figure 1 Geometry used for theoretical development.

The total field at the receiver is the sum of a direct field contribution, a contribution from the plane boundary and a contribution from the cylindrical scatterers and must satisfy the Helmholtz equation

$$\nabla^2 P + k_0^2 P = 0 \quad (1)$$

Assuming a direct field represented by a Hankel function  $H_0(k_0\rho)$  where  $k_0$  is the wave-number exterior to the cylinders and  $\rho$  is the source-receiver distance, a plane boundary reflected wave  $H_0(k_0\rho')$  taken into account by assuming an image source, a scattered field decomposed into a sum of the contributions from the  $N$  cylinders and  $N$  cylinder images, the following expression can be developed for the total field above the array of cylinders

$$\begin{aligned} P = & \sum_{n=-\infty}^{+\infty} J_n(k_0 r_j) H_n^{(1)}(k_0 S_j) e^{-in\sigma_j} e^{in\theta_j} + \sum_{n=-\infty}^{+\infty} J_n(k_0 r'_j) H_n^{(1)}(k_0 S'_j) e^{-in\sigma'_j} e^{in\theta'_j} \\ & + \sum_{j=1}^N \sum_{n=-\infty}^{\infty} A_n^j Z_n^j H_n^{(1)}(k_0 r_j) e^{in\theta_j} + \sum_{j=1}^N \sum_{n=-\infty}^{\infty} A_n^j Z_n^j H_n^{(1)}(k_0 r'_j) e^{in\theta'_j} \\ & + \sum_{j=1, j \neq s}^{2N} \sum_{n=-\infty}^{\infty} A_n^j \sum_{m=-\infty}^{\infty} J_m(k_0 r_s) H_{n-m}^{(1)}(k_0 r_{js}) e^{i(n-m)\alpha_{js}} \end{aligned} \quad (2)$$

Provided that  $r_j < S_j$  and  $r_j < S'_j$ . Here  $J_n$  are Bessel functions of order  $n$  and  $H_n^{(1)}$  are Hankel functions of the first kind and order  $n$ .  $A_n^j$  are unknown amplitudes and  $\alpha_{js}$  is 0 or  $\pi$  depending on the relative positions of the  $j$ th and  $s$ th cylinders.

For acoustically rigid cylinders of radii  $a$  the term  $Z_n^j$  is defined as

$$Z_n^j = \frac{J'_n(k_0 a)}{H'_n(k_0 a)} \quad (3)$$

where  $J'_n()$  and  $H'_n()$  are derivatives of the Bessel and Hankel functions, respectively. The application of Graf's addition theorem for Bessel functions has also been used to express  $H_n^{(1)}(k_0 r_j)$  and  $H_n^{(1)}(k_0 r'_j)$  in terms of the coordinates  $(r_j, \theta_j)$  and  $(r'_j, \theta'_j)$ .

The application of boundary conditions leads to an infinite system of equations for unknown coefficients  $A$ :

$$A_m^S + \sum_{\substack{j=1 \\ j \neq s}}^{2N} \sum_{n=-\infty}^{\infty} A_n^j Z_n^j H_{n-m}^{(1)}(k_0 R_{js}) e^{i(n-m)\alpha_{js}} = -H_m^{(1)}(k S_{p1}) e^{-im\sigma_{p1}} - H_m^{(1)}(k S_{p2}) e^{-im\sigma_{p2}} \quad (4)$$

with  $m \in Z$  and  $S = 1, \dots, 2N$ . The summation includes cylinders and their images thus taking the total number of elements to  $2N$ . The source terms on the right-hand side are the source and its image below the rigid plane. To determine the coefficients  $A_n^j$ , the infinite summation is truncated to  $-M$  to  $M$  resulting in a system of  $2N(2M + 1)$  equations. The value of  $M$  is set to 6 (for further details see [14]). The procedure for determining the total field at a certain point using this multiple scattering approach requires solving the system of equations (4) and determining the pressure by summation using equation (2) together with direct and boundary-reflected terms. This procedure has been implemented using MatLab.

### 3 NUMERICAL PREDICTIONS

The scattering of acoustic pulses of infinitely short length, corresponding to a flat, infinitely-wide, frequency spectrum, from the cylinder array is determined from the convolution of  $P$  with the Dirac delta function

$$P_{Ref}(t) = \begin{cases} 1, & t = 0 \\ 0, & otherwise \end{cases} \quad (5)$$

The advantage of using such a pulse in simulations is that the response in the frequency domain is independent of frequency content of the input pulse.

Figure 2 shows the results of time and frequency domain simulations for two different cylinder array configurations. In the first, cylinders are positioned regularly and symmetrical about the point of specular reflection at a cylinder centre-to-centre spacing of 5 cm, corresponding to 20 cylinders between source and receiver. In the second, 20 cylinders are arranged irregularly between source and receiver. The source-receiver separation is 1 m and both the source and receiver heights are 5 cm. In both configurations, a main pulse arrival at 2.9 ms (corresponding to a sound speed of 343 m/s) is followed by a "tail" which persists for some time after the main pulse. In the regular arrangement, this persistence is for some 5 to 10 ms. The spectrum of this tail is dominated by a peak at 2.7 kHz and three other peaks at 5.8 kHz, 9.6 kHz and 13.6 kHz with much lower magnitudes. This contrasts with the simulations for the irregular array: the tail dies out within some 2 ms and its spectrum, although containing a peak (albeit at a lower magnitude) equivalent to the peak at 2.7 kHz in the regular arrangement, does not have any of the peaks at higher frequencies.

Clearly, the regularity of the cylinder array has an impact on the frequency content of the pulse tail and must consequently be generating a coherent field in the vicinity of the array. To understand better

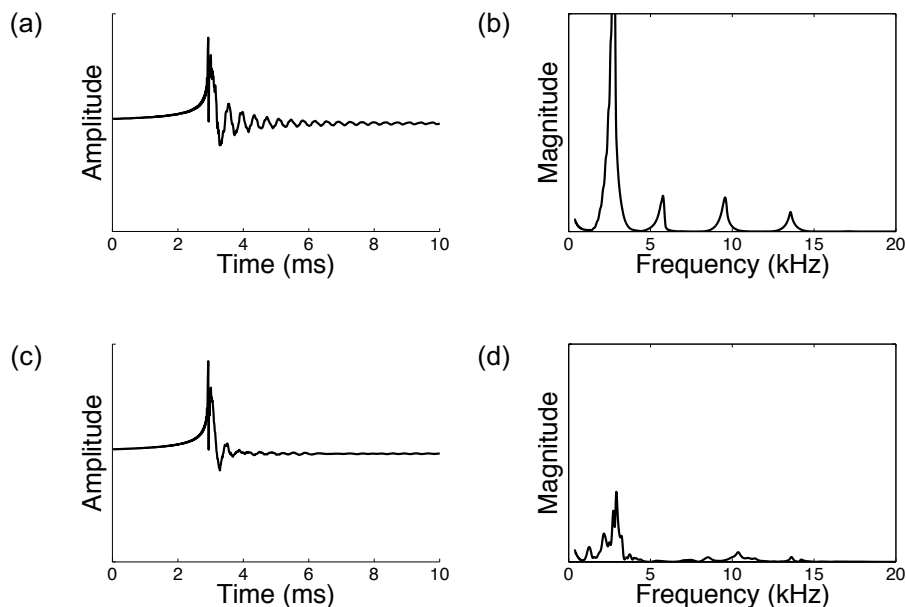


**Figure 2** Example pulses and tail spectra calculated for propagation over cylinder array (20 cylinders, diameter 1.5 cm) for an input delta pulse. Source-receiver separation = 1.0 m, source and receiver heights  $h_s = h_r = 5$  cm: (a) and (b) regular arrangement, cylinder centre-to-centre spacing 5 cm, (c) and (d) irregular arrangement.

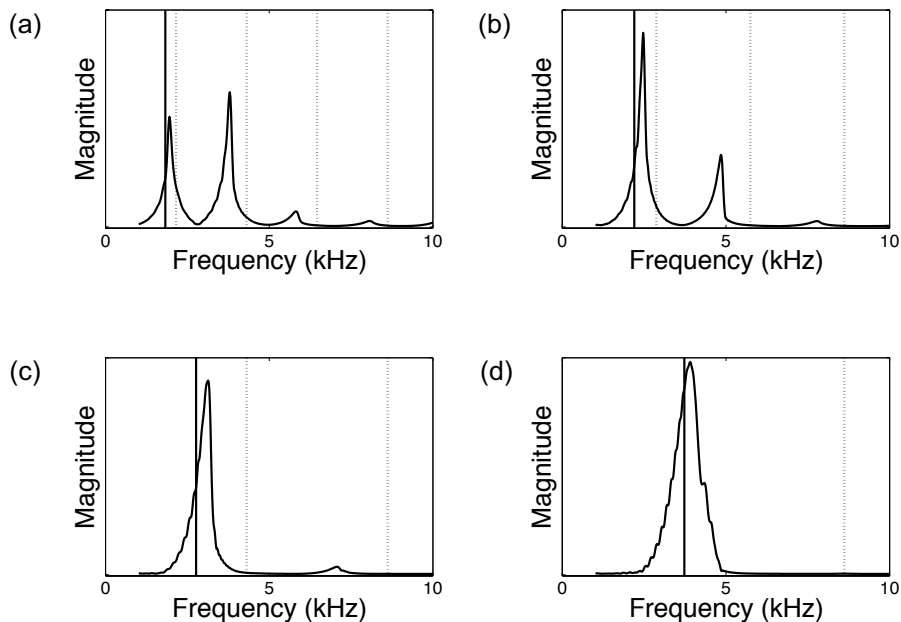
what mechanisms are generating this field, let us consider the effects of altering cylinder centre-to-centre spacing and cylinder size.

Figure 3 shows pulse tail spectra as a function of cylinder centre-to-centre spacing for a fixed cylinder diameter (1.5 cm). It can be seen that with decreasing cylinder-to-cylinder separations (i.e., increasing the number of cylinders between the source and receiver), the spacing between the peaks in the spectra increases so much so that for compact cylinder array (2 cm cylinder-to-cylinder spacing) the spectrum is dominated by only one peak. In general, these peaks approximately correspond to the Bragg interference frequencies (the dotted lines) given by

$$f_{br} = \frac{c_0 n}{2R \sin \gamma}, n = 1, 2, 3, \dots \quad (6)$$

where  $c_0$  is the speed of sound in air,  $R$  is the cylinder centre-to-centre spacing and  $\gamma$  is the angle of incidence (angle with the normal of surface reflected wave at point of specular reflection). This assumes the scattering elements to be of infinitesimal size and, therefore, that the Bragg frequency is independent of the size of the scattering elements.

However, this is not the case for the first peak and it is proposed here that for small cylinder-to-cylinder spacings, a different mechanism starts to dominate the spectra at approximately the same frequency as the first order Bragg diffraction maxima.



**Figure 3** Spectra of pulse tails calculated over a cylinder array (cylinder diameter 1.5 cm) for cylinder centre-to-centre spacings (a) 8 cm, (b) 6 cm, (c) 4 cm and (d) 2 cm for an input delta pulse. The source-receiver separation = 1.0 m, source and receiver heights  $h_s = h_r = 5$  cm. Also shown for each array is the 1st organ-pipe resonance frequency (solid line) and the 1st and subsequent order Bragg diffraction frequencies (dashed lines).

The gaps between the cylinders may be considered to act as “organ pipes”, closed at one end. A cylindrical organ pipe of length  $L$  and diameter  $d$  has (quarter wavelength) resonances given by

$$f_{OP} = \frac{c_0 n}{4(L + 0.4d)}, n = 1, 3, 5, \dots \quad (7)$$

With the length of the “organ pipe” taken to be  $L = 2a$ , where  $a$  is the cylinder radius of the array and its effective diameter taken to be  $d = R$ , where  $R$  is the cylinder centre-to-centre spacing then the frequency of the first “gap” resonance is

$$f_{OP}^1 = \frac{c_0}{4(2a + 0.4R)}. \quad (8)$$

The solid line in Figure 3 shows this frequency and demonstrates good agreement over the range of cylinder-to-cylinder spacings.

Further confirmation of the latter effect can be made if we consider the predicted tail spectra as a function of cylinder diameter for a fixed cylinder centre-to-centre spacing. Figure 4 shows that with increasing cylinder diameters, the first peak in the spectra migrates to lower frequencies which is in fact reflected in the changing frequency of the organ-pipe resonance. As the Bragg diffraction frequencies are not cylinder size dependent, their frequencies (indicated as the dotted lines in the figures) do not alter.

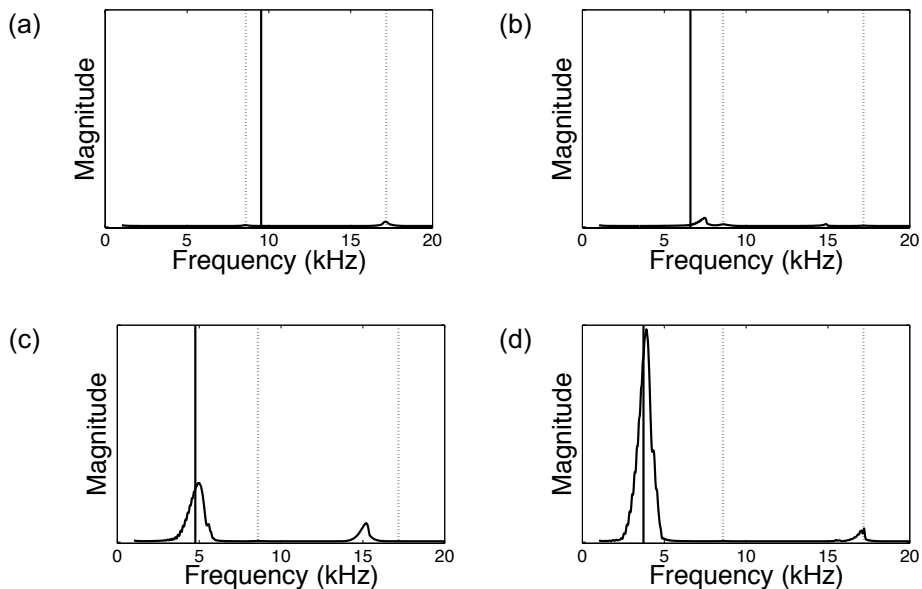


**Figure 4** Spectra of pulse tails calculated over a cylinder array with cylinder centre-to-centre spacing of 5 cm for cylinder diameters (a) 1.0 mm, (b) 5 mm, (c) 10 mm, (d) 15 mm for an input delta pulse. The source-receiver separation = 1.0 m, source and receiver heights  $h_s = h_r = 5$  cm. Also shown for each array is the 1st organ-pipe resonance frequency (solid line) and the 1st and subsequent order Bragg diffraction frequencies (dashed lines).

Finally, let us the total field generated at points in the vicinity of the cylinder array at the frequency of the first spectral peak. Figure 5 shows a map of the total pressure magnitude up to 10 cm above an array of 20 1.5 cm cylinders with centre-to-centre spacing of 5 cm for the frequency 2782 Hz (corresponding to the frequency of first peak in the tail spectrum for this configuration. It also shows a map for double the number of cylinders (4).

In both cases, the “organ-pipe” gap resonance effect increases the pressure magnitude between the cylinders. There also seems to be some kind of “standing-wave” envelope, could be confined to a region just above the cylinders. This effect however is not present in the more compact configuration. Furthermore, test have shown that the field decreases exponentially with height above the array.

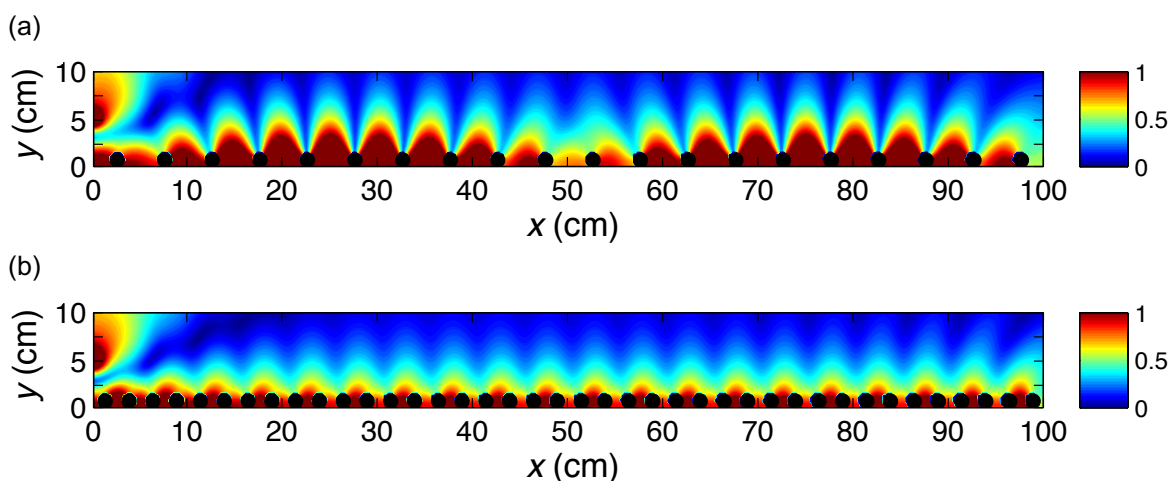


**Figure 5** Pressure maps calculated above cylinder array with cylinder centre-to-centre spacing of (a) 5 cm (20 cylinders) for frequency 2782 Hz and (b) 2.5 cm (40 cylinders) for frequency 3169 Hz, cylinder diameter 1.5 cm for an input delta pulse. The source-receiver separation = 1.0 m, the source height  $h_s = 5$ .

## 4 DISCUSSION

Using predictions of a multiple scattering theory for propagation from a cylindrical source close to an array of cylinders on a rigid plane, we have shown that pulses received, also close to the surface, are composed of a main arrival and a tail. A spectral analysis of the tail demonstrates that it is composed of regularly-spaced frequency components that correspond to plane-wave Bragg diffraction. However, at small cylinder centre-to-centre spacings, these components are weak in comparison to a strong low frequency component related to the quarter wavelength “organ pipe” or “gap” resonance in the spacing between the cylinders and which, in turn, is enhanced with increasing cylinder diameter. Pressure maps show resonances between neighbouring cylinders and an interaction between the gap resonances just above the cylinder array.

In their study of the propagation of pulses over lattices, Daigle et al [17] and found that, at source-receiver separations greater than 1.5 m, there is a clear time lag between the main arrival and the tail of ~10-15 ms. In the present study of the propagation of pulses over cylinders on a rigid surface, albeit a rather different type of irregular rough surface, we have not been able to demonstrate a separation of the pulse tail from the main arrival, using the multiple scattering theory. This implies that the surface wave created by the cylinders on a hard plane has a speed rather close to the speed of sound in air. Given the tail’s dependence upon interference and resonance effects for its generation,

it cannot be considered an independently propagating wave. As such, can this wave be considered a *surface wave*, in the same sense as a Rayleigh wave observed in elastic media?

## 5 ACKNOWLEDGMENTS

This research was developed while DLB was a Visiting Fellow at the Open University, on sabbatical leave from the University of Évora during the academic year 2017-18; support from the Open University and the Foundation for Science and Technology (Fundação para a Ciência e a Tecnologia), Portugal, reference SFRH/BSAB/135168/2017, is gratefully acknowledged.

## 6 REFERENCES

1. S. Thomasson, 'Reflection of waves from a point source by an impedance boundary', *J. Acoust. Soc. Am* 59(4), 780-785. (1975).
2. R. Raspet and G. E. Baird, 'The acoustic surface wave above a complex impedance ground surface', *J. Acoust. Soc. Am.* 85, 638–640. (1989).
3. I. Tolstoy, 'Coherent sound scatter from a rough interface between arbitrary fluids with particular reference to roughness element shapes and corrugated surfaces', *J. Acoust. Soc. Am.* 72, 960–972. (1982).
4. I. Tolstoy, 'Smoothed boundary conditions, coherent low-frequency scatter, and boundary modes', *J. Acoust. Soc. Am.* 72, 1–22. (1983).
5. V. Twersky, 'Reflection and scattering of sound by correlated rough surfaces', *J. Acoust. Soc. Am.* 73, 85– 94. (1983).
6. K. M. Ivanov-Shits and F. V. Rozhin, 'Investigation of surface waves in air', *Sov. Phys. Acoust.* 5, 510–512. (1959).
7. R. J. Donato, 'Model experiments on surface waves', *J. Acoust. Soc. Am.* 63, 700–703. (1978).
8. I. Bashir, S. Taherzadeh, and K. Attenborough, 'Surface waves over periodically-spaced strips'. *J. Acoust. Soc. Am.* 134 (6) 4691 – 4697. (2013).
9. W. Zhu, M. Stinson, and G. A. Daigle 'Scattering from impedance gratings and surface wave formation', *J. Acoust. Soc. Am.* 111, 1996–2012. (2002).
10. W. Zhu, G. A. Daigle, and M. Stinson, 'Experimental and numerical study of air-coupled surface waves generated above strips of finite impedance', *J. Acoust. Soc. Am.* 114, 1243–1253. (2003).
11. W. Lauriks, L. Kelders, and J. F. Allard 'Surface waves above gratings having a triangular profile', *Ultrasonics* 36, 865–871. (1998).
12. L. Kelders, J. F. Allard, and W. Lauriks, 'Ultrasonic surface waves above rectangular-groove gratings', *J. Acoust. Soc. Am.* 103, 2730–2733. (1998).
13. J. F. Allard, L. Kelders, and W. Lauriks 'Ultrasonic surface waves above doubly-periodic grating', *J. Acoust. Soc. Am.* 105, 2528–2531. (1999).
14. P. Boulanger, K. Attenborough, Q. Qin and C.M. Linton, 'Reflection of sound from random distributions of semi- cylinders on a hard plane- models and data', *J. Phys. D: Appl. Phys.* 38 3480–3490. (2005).
15. I Bashir, TJ Hill, S Taherzadeh, K Attenborough and M Hornix, 'Reduction of surface transport noise by ground roughness', *Appl. Acoustics*, 83(1), 1-15. (2014).
16. C. M. Linton and V. Evans, 'The interaction of waves with arrays of vertical circular cylinders', *J. Fluid Mech.* 215, 549–69. (1990).
17. G. A. Daigle, M.R. Stinson and D.I. Havelock, 'Experiments on surface waves over a model impedance plane using acoustical pulses', *J. Acoust. Soc. Am.* 99 (4), Pt. 1. (1996).